10.5005/jp-journals-10025-1120

CASE REPORT

Unilateral Ectasia characterized by Advanced Diagnostic Tests

[1-3]Isaac C Ramos, [4-7]Dan Z Reinstein, [4]Timothy J Archer, [4]Marine Gobbe, [2,3,15]Marcella Q Salomão, [2,3,15]Bernardo Lopes [2,3,15]Allan Luz, [2,10-12]Fernando Faria-Correia, [13]Damien Gatinel, [14]Michael W Belin, [2,3,8,9,15]Renato Ambrósio Jr

ABSTRACT

To describe a case of very asymmetric ectasia successfully treated by femtosecond laser-assisted intracorneal ring segment implantation, in which the diagnosis of unilateral ectasia in the right eye was based on the clinical findings including history, follow-up, and advanced diagnostic data. The patient's history was positive for ocular allergy with moderate-to-intense eye rubbing only in the right eye. The uncorrected distance visual acuity was 20/63 in the right eye and 20/32 in the left eye. The corrected distance visual acuity (CDVA) was 20/40 in the right eye (−1.75−4.00×35°) and 20/16 in the left eye (−0.50−0.25×115°). After femtosecond laser-assisted intracorneal ring segment implantation, the right eye improved CDVA to 20/20^{-1}. Concerning ectasia/keratoconus diagnosis, the left eye remained stable over 1 year of follow-up with unremarkable topometric, tomographic, and biomechanical findings. Epithelial thickness mapping by spectral domain optical coherence tomography and very-high-frequency digital ultrasound demonstrated epithelial thickness within normal limits in the left eye. Advanced diagnostic methods along with clinical data enable the distinction from unilateral ectasia cases and subclinical (fruste) keratoconus. Literature review is also performed along with case presentation and discussion.

Keywords: Corneal tomography, Keratoconus, Unilateral ectasia.

How to cite this article: Ramos IC, Reinstein DZ, Archer TJ, Gobbe M, Salomão MQ, Lopes B, Luz A, Faria-Correia F, Gatinel D, Belin MW, Ambrósio R Jr. Unilateral Ectasia characterized by Advanced Diagnostic Tests. Int J Kerat Ect Cor Dis 2016;5(1):40-51.

Source of support: Nil

Conflict of interest: Drs. Ambrósio and Belin are consultants for Oculus (Wetzlar, Germany); Dr. Reinstein is a consultant for Carl Zeiss Meditec (Carl Zeiss Meditec AG, Jena, Germany) and has proprietary interest in the Artemis technology (ArcScan Inc, Morrison, Colorado, USA) through patents administered by the Center for Technology Licensing at Cornell University (CTL), Ithaca, New York, USA. Dr. Gatinel is a consultant for TECHNOLAS Perfect Vision (Munich, Germany). The remaining authors have no proprietary or financial interest in the materials presented herein.

[1-3]Research Associate, [4-7]Professor, [4]Research Associate [4]Research Associate, [2,3,15]Research Associate, [2,3,15]Research Associate, [2,3,15]Research Associate, [2,10-12]Research Associate [13]Professor, [14]Professor, [2,3,8,9,15]Professor

[1]Hospital de Olhos Santa Luzia, Maceió, Alagoas, Brazil

[2]Rio de Janeiro Corneal Tomography and Biomechanics Study Group, Rio de Janeiro, Brazil

[3]Brazilian Study Group of Artificial Intelligence and Corneal Analysis – BRAIN, Maceió, Alagoas, Brazil

[4]London Vision Clinic, London, UK

[5]Department of Ophthalmology, Columbia University Medical Center, Columbia, New York, USA

[6]Centre Hospitalier National d'Ophtalmologie, Paris, France

[7]Biomedical Science Research Institute, University of Ulster Coleraine, Northern Ireland

[8]Instituto de Olhos Renato Ambrósio, Rio de Janeiro, Brazil

[9]VisareRIO, Refracta Personal Laser, Rio de Janeiro, Brazil

[10]Life and Health Sciences Research Institute, School of Health Sciences, University of Minho, Braga, Portugal

[11]ICVS/3B's-PT Government Associate Laboratory, Braga/Guimarães, Portugal

[12]Department of Ophthalmology, Hospital de Braga, Braga Portugal

[13]l'Institut Laser Vision, Fondation Ophtalmologique A. de Rothschild, Paris, France (Fondation Rothschild)

[14]Department of Ophthalmology and Vision Science, University of Arizona, Tucson, Arizona, USA

[15]Department of Ophthalmology, Federal University of São Paulo, São Paulo, Brazil

Corresponding Author: Renato Ambrósio Jr, Rua Visconde de Pirajá 550/1701 – Ipanema,Rio de Janeiro 22410-002, Brazil e-mail: dr.renatoambrosio@gmail.com

INTRODUCTION

Keratoconus is the most common ectatic corneal disorder, which typically presents bilaterally but at times can present with a high degree of asymmetry.[1,2] Interestingly, some cases with very high asymmetry between eyes may present with a relatively normal corneal front surface curvature in the less affected eye. Such cases have previously been reported as "unilateral keratoconus" with an incidence ranging between 1 and 4%.[3-6] However, both the pan-American and global consensus on keratoconus and corneal ectatic diseases concluded that "true unilateral keratoconus does not exist" based on the assumption there is a genotype for this condition, albeit with incomplete penetrance.[7,8] In fact, Klyce[9] referred such fellow eyes with normal topography as "*forme fruste* keratoconus," instead of "unilateral keratoconus" cases. *Forme fruste* keratoconus was originally coined by Amsler[10] for

describing the incomplete or abortive form of the disease that may or may not progress, mostly depending on external influences, to the full-blown (*forme plaine*) disease at some point in the future. As Amsler[10] demonstrated using predigital photokeratoscopy analysis, other longitudinal studies have demonstrated that many of Forme fruste keratoconus fellow eyes progressed to true keratoconus over the long term. For example, Suzuki et al[11] found that 20% of eyes progressed within 6 years.

There are, however, some cases in which the ectatic process only occurs in one eye, having no feature of ectatic corneal disease in the fellow eye. For such cases, there was consensus that secondary (induced) ectasia may be caused by a pure mechanical process.[7,8] These concepts are based on the current two-hit hypothesis that proposes ectasia development can occur in patients with an underlying genetic predisposition, but only when coupled with external environmental factors,[12] including eye rubbing,[13,14] ocular trauma, rigid contact lens wear, and the weakening caused by keratorefractive surgery.[15,16]

The challenge is that distinguishing unilateral ectasia from very asymmetric keratoconus can only be proved by collecting longitudinal data to confirm whether ectasia progression will occur or not.[5] It appears likely that some cases may simply not progress unless there is a significant destabilizing hit provided by an environmental stimulus. However, this is as distinct from a patient with keratoconus, in which the ectatic progression can occur without any external environmental factors, although such factors will obviously accelerate progression.

Advanced diagnostic corneal imaging technologies (e.g., corneal tomography) have been proven to augment the sensitivity to detect mild abnormalities related to ectasia[16,17] and epithelial thickness mapping.[18-20] When evaluating these diagnostic techniques, many researchers have used eyes with normal or relatively normal topographic findings from patients with very asymmetric ectasia, based on the assumption that keratoconus is a bilateral disease and therefore the fellow eye must have a mild form.[21-27] These studies have proven to vary in results, with some demonstrating much higher diagnostic sensitivity than others; however, this may be due to the different criteria for defining abnormal front surface topography. Some studies included fellow eyes with some suspicious signs on topography,[28] whereas others included only fellow eyes with normal topography.[21-27] For example, a recent study by Reinstein et al[27] found that only half of the fellow eyes with normal clinical and topographical evaluation from 10 patients with very asymmetric ectatic disease had detectable abnormalities characteristic of keratoconus by advanced diagnostic techniques, including epithelial thickness mapping,[29] Belin-Ambrósio[30] enhanced ectasia display, and the SCORE algorithm developed by Gatinel and Saad.[21,31] It seems possible that at least some of these patients are more likely to be cases of unilateral secondary induced ectasia, or cases with false positive topography in the so-called affected eye, rather than patients with asymmetric keratoconus.

The current case report describes a patient with unilateral ectasia in which the exclusion of subclinical (or *forme fruste*) keratoconus was done based on extensive advanced diagnostic tests, along with a critical evaluation of clinical history.

CASE REPORT

A 39-year-old business executive was referred for specialized keratoconus treatment to VisareRIO (Rio de Janeiro, Brazil). The patient complained of low vision in his right eye and reported ocular allergy with moderate-to-intense itching and eye rubbing only in the right eye. The uncorrected distance visual acuity was 20/63 in the right eye and 20/32 in the left eye. Wavefront-facilitated manifest refraction was –1.75–4.00×35° in the right eye and –0.50 –0.25×115° in the left eye. Corrected distance visual acuity (CDVA) was 20/40 in the right eye and 20/16 in the left eye.

Placido disk-based corneal topography was obtained by Keratograph 5 (Oculus, Wetzlar, Germany) and iTrace (Tracey Technologies, Houston, USA), and Scheimpflug corneal tomography was performed using the Pentacam HR (Oculus, Wetzlar, Germany). Front surface curvature maps by Placido (Figs 1A, B and 2) were identical to those generated by rotating Scheimpflug corneal tomography (Figs 1C and D) in both eyes. A marked irregularity with steep and truncated bowtie and skewed radial axis was noted in the right eye (Figs 1A, C and 2A). The left eye had a relatively normal asphericity with low astigmatism (Figs 1B, D and 2B). Oculus topometric keratoconus classification (TKC)[32,33] was consistent with grade 2 keratoconus in the right eye and had no similarity with ectatic disease in the left eye. The Belin ABCD keratoconus staging A2B2C0D1 in the right eye and A0B0C0D0 in the left eye[34] was determined.

Ocular wavefront analysis was done by the iTrace (Figs 2C and D), demonstrating a similar pattern of irregularity as seen on front surface curvature in the right eye. Central wavefront refraction was –0.75–4.25 × 35° in the right eye and –0.37–0.12 × 24° in the left eye. The total high-order aberrations (HOAs) were 0.472 µm in the right eye and 0.099 µm in the left eye for 3.2 mm pupil diameter scan.

Figures 3 and 4 include the enhanced tomographic evaluation by Pentacam HR for OD and OS respectively. Figure 3 revealed an ectatic pattern in the elevation maps for the front and back surfaces in the right eye. Pachymetric distribution graphs (corneal thickness special profile and percentage of thickness increase)[35] demonstrated a

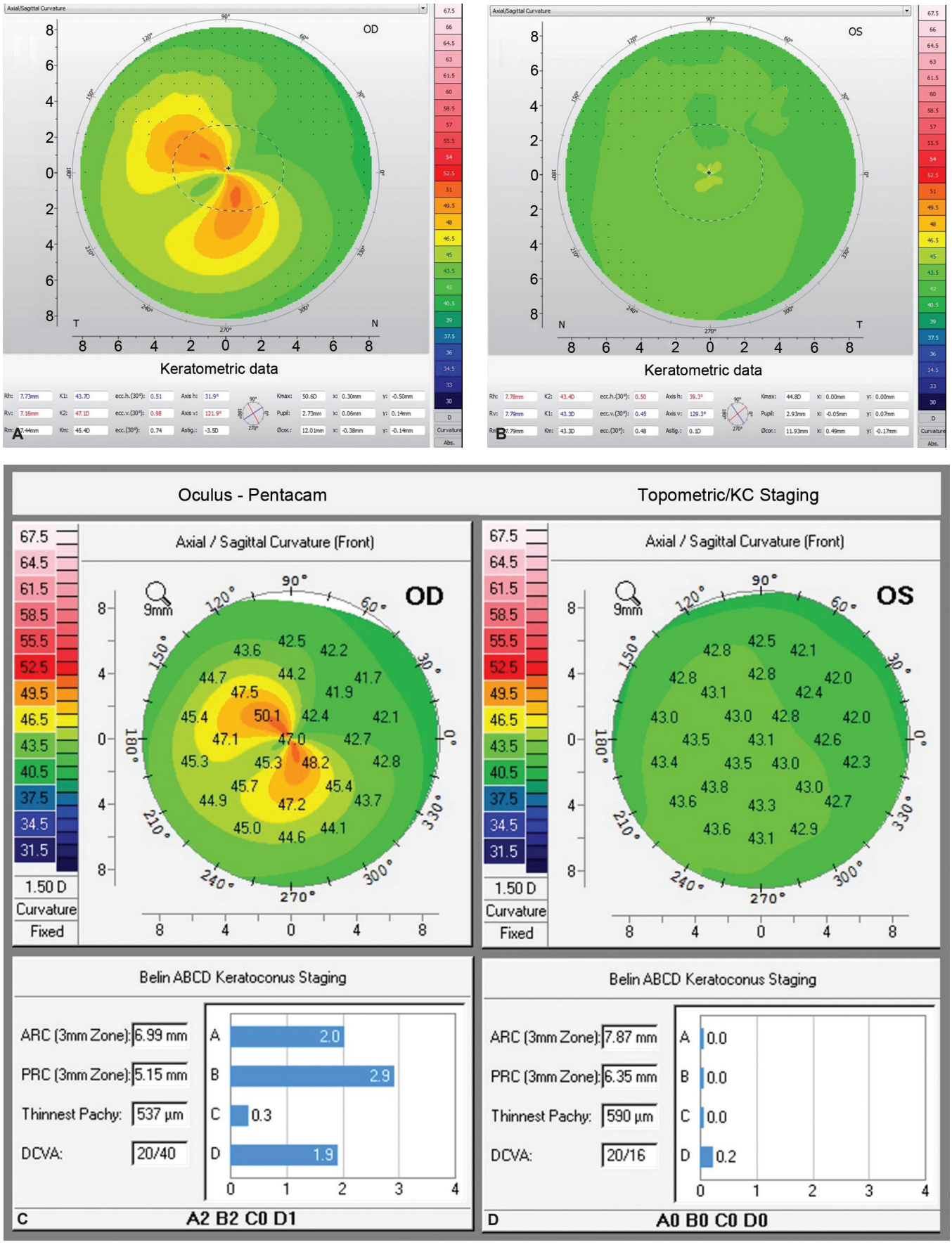

Figs 1A to D: Keratograph 5 (A and B), and Pentacam HR (C and D) front surface axial curvature (topometric) maps, including Belin ABCD keratoconus staging

Figs 2A to D: iTrace summary with axial curvature (A and B), and ocular wavefront data (C and D)

pattern of abrupt increase in thickness from the thinnest point outward in the right eye (Fig. 3).[36] In the right eye, the elevation for a best-fit sphere in an 8-mm zone in the location of the thinnest point was 18 µm for the front surface and 47 µm for the back surface. Elevation and pachymetric maps, along with pachymetric distribution graphs, were unremarkably normal in the left eye (Fig. 4). ARTmax (Ambrósio Relational Thickness to the meridian with maximal pachymetric increase) was 240 µm in the right eye and 535 µm in the left eye.[36] BAD-D version 3 (Belin-Ambrósio Deviation index) was 5.25 in the right eye and 0.25 in the left eye.

Figure 5 illustrates the layered pachymetric mapping by spectral domain optical coherence tomography (OCT) done using the RTVue (Optovue; Fremont, CA, USA). The total pachymetric map findings were similar to those generated by Pentacam HR. The thinnest value was displaced toward the inferotemporal quadrant in both eyes. The minimum pachymetry in the right eye was 539 µm by OCT and 537 µm by Scheimpflug, whereas

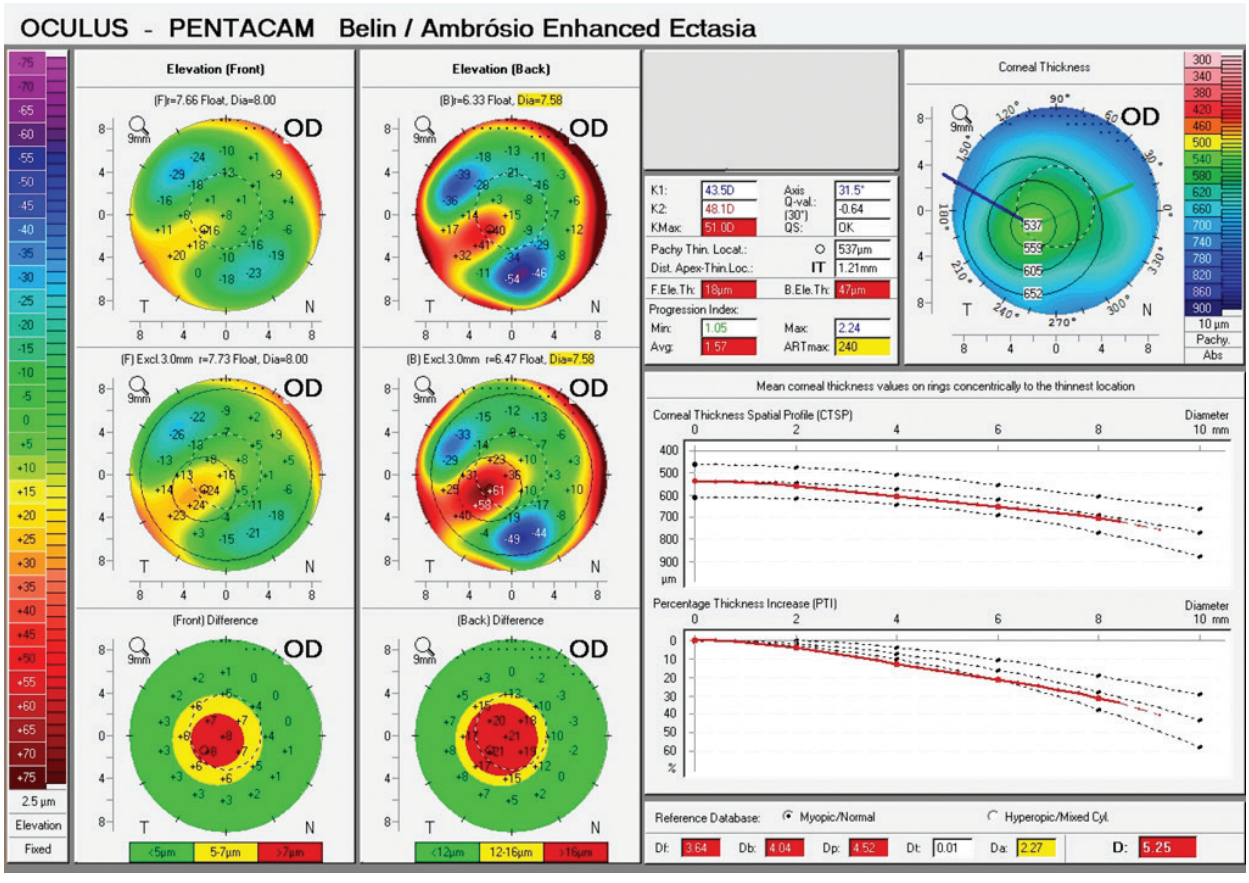

Fig. 3: Enhanced ectasia display from OD

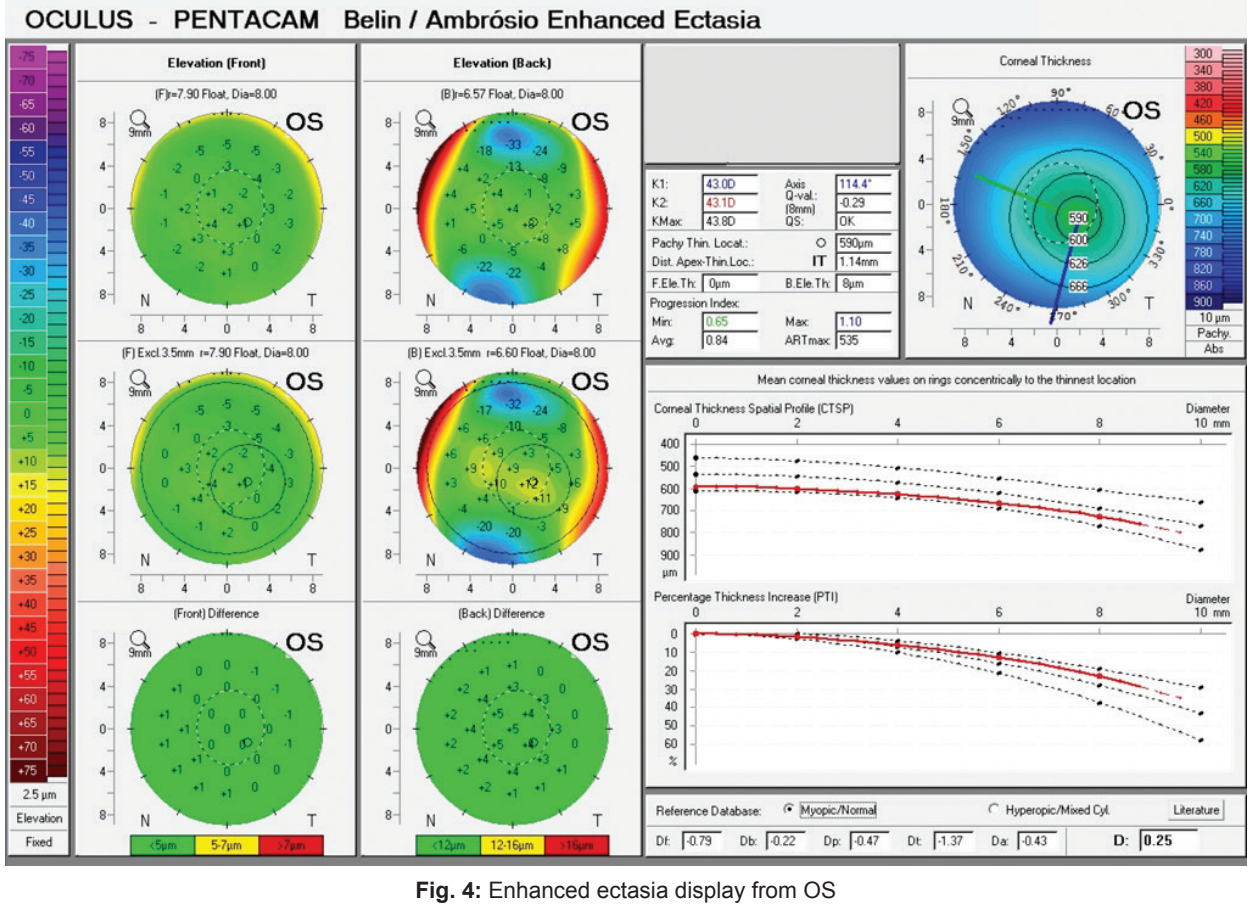

Fig. 4: Enhanced ectasia display from OS

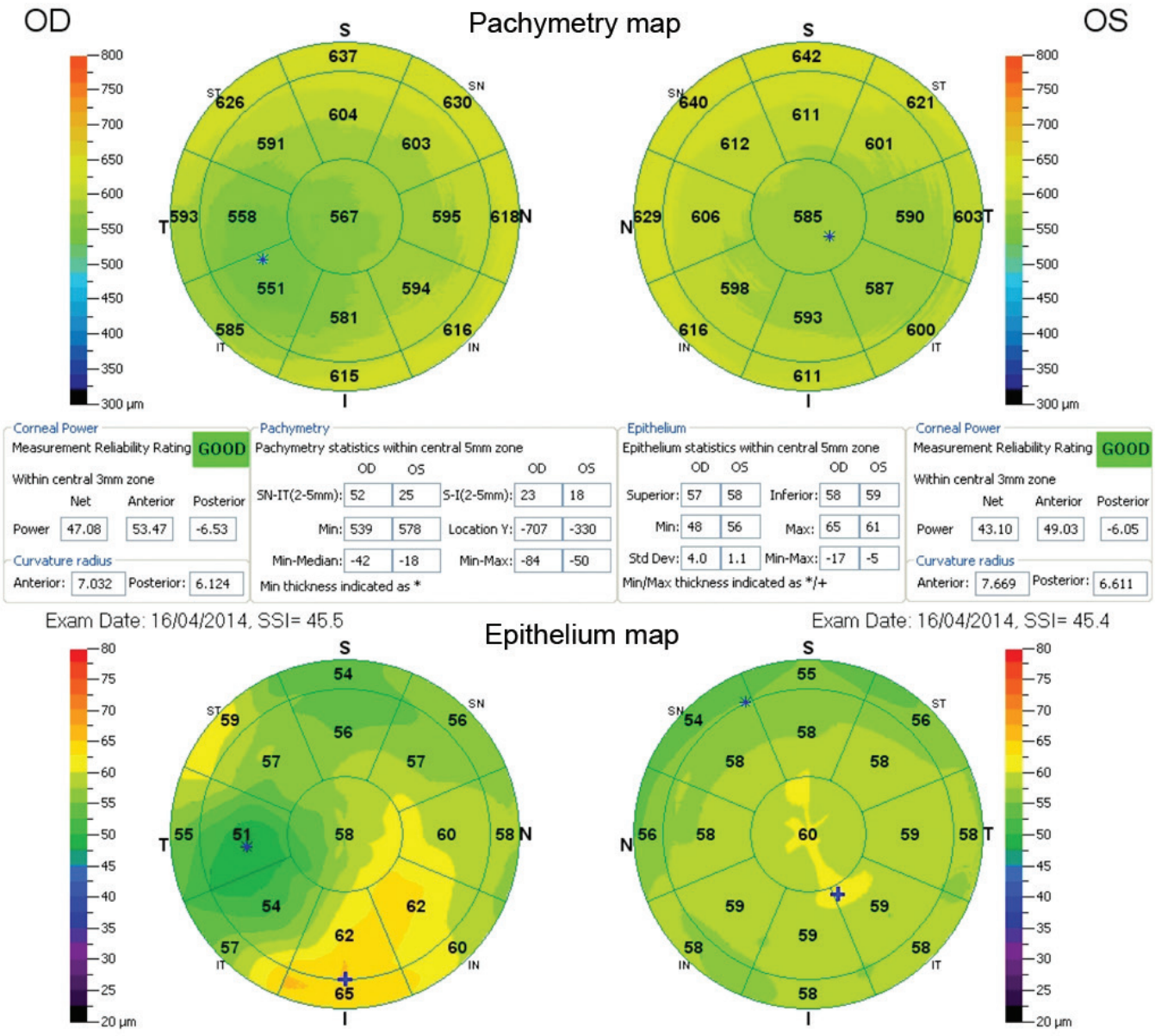

Fig. 5: Layered pachymetric mapping from optical coherence tomography

the minimum pachymetry in the left eye was 578 µm by OCT and 590 µm by Scheimpflug. In the right eye, the epithelial thickness map provided by OCT demonstrated a region of thinner epithelium inferotemporally, surrounded by thicker epithelium, and was coincident with the thinnest area on pachymetry and the apex on front and back surface elevation maps. The epithelial thickness map was found to be relatively normal in the left eye.

Corneal endothelium was evaluated by specular microscopy (Tomey; Nagaya, Japan) with a normal mosaic and central count of 2,495 cells/mm^2 in the right eye and 2,590 cells/mm^2 in the left eye. The Ocular Response Analyzer[37] (ORA; Reichert, Buffalo, NY, USA) and Corvis ST[38] (Oculus, Wetzlar, Germany) (Figs 6A and B) were used to assess ocular biomechanical properties. A relatively low-signal applanation response was observed in the right eye and a normal response was observed in the left eye.[39] Corneal hysteresis (CH) and corneal resistance factor (CRF) were 8.8 and 8.1 mm Hg in the right eye and 12.1 and 12.0 mm Hg in the left eye.

The diagnosis of unilateral ectasia in the right eye was based on the clinical findings along with tomographic data from both eyes. Considering the patient's symptoms and clinical findings, the treatment plan was to implant intracorneal ring segments (ICRSs) assisted by femtosecond laser in the right eye. Based on the Mediphacos nomogram 4.0 (Belo Horizonte, Brazil), one segment of Keraring SI6 150° with 250 µm was implanted temporally with an incision at the steepest meridian with depth calculated at 80% of minimal pachymetric value. The FS-200 femtosecond laser (Alcon-WaveLight; Earlagen, Germany) was used to create tunnels. Surgical procedure and postoperative period occurred with no complications.

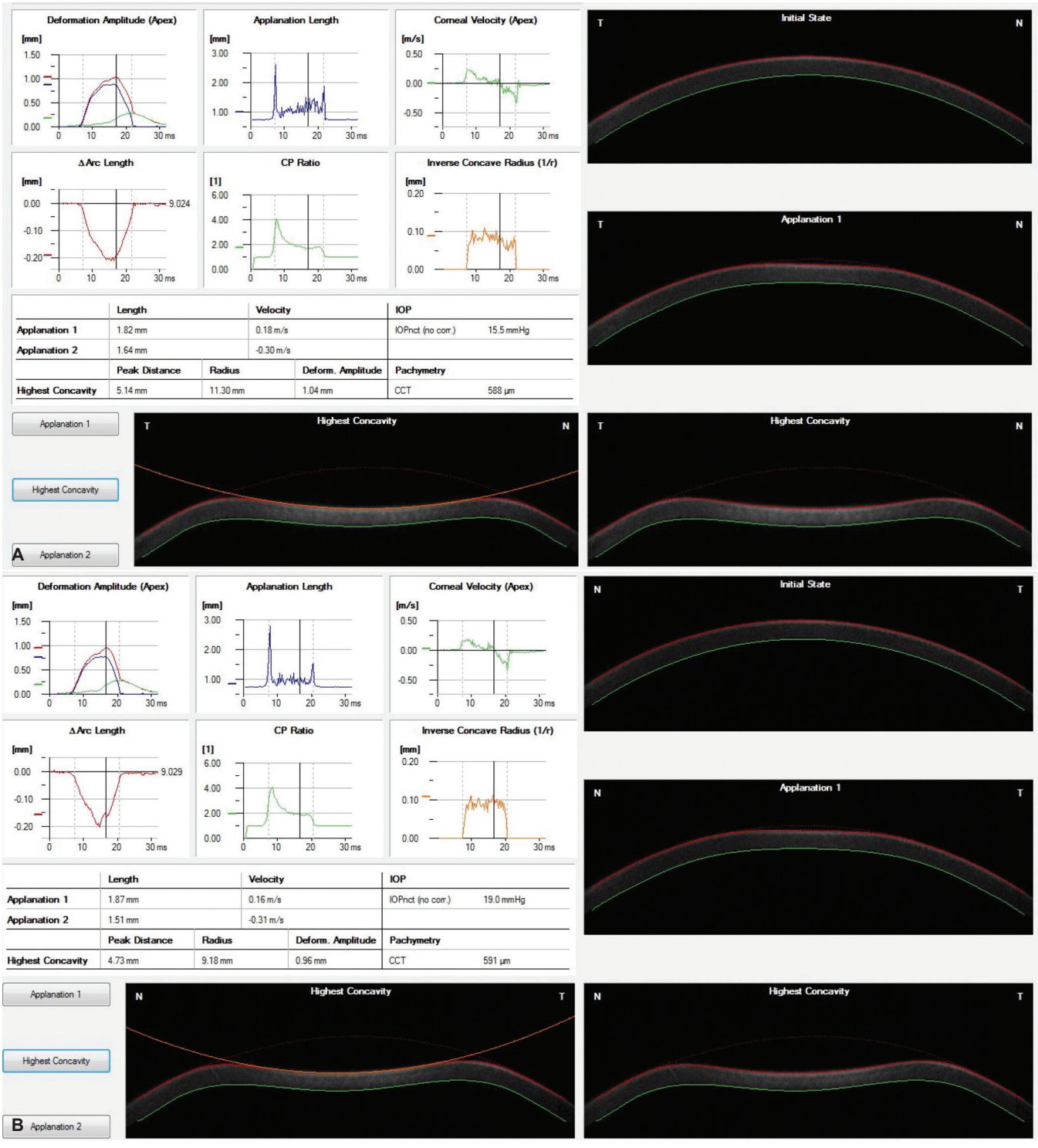

Figs 6A and B: Corvis ST from OD (A), and OS (B)

The patient noticed an improvement in his quality of vision since 1 week after surgery. Six weeks after surgery, the ICRS was in position without ocular inflammation (Fig. 7). Uncorrected distance visual acuity was 20/50- and manifest refraction was –2.00–0.50×140°, giving CDVA of 20/20. A marked improvement in corneal irregularity was noted on corneal topography (Fig. 8). The main keratometric changes in this eye were the decrease in K_{max} from 51.0D to 47.8D and keratometric central astigmatism from 4.6DC to 0.2DC in the right eye (Fig. 8).

The patient moved to London, UK, due to his career and was referred to the London Vision Clinic for clinical follow-up with Prof. Dan Z. Reinstein. One year after surgery, he presented with relatively stable clinical findings in both eyes accordingly to his last examination. Corrected distance visual acuity was 20/20-1 in the right eye and 20/16 left eye. In this visit,

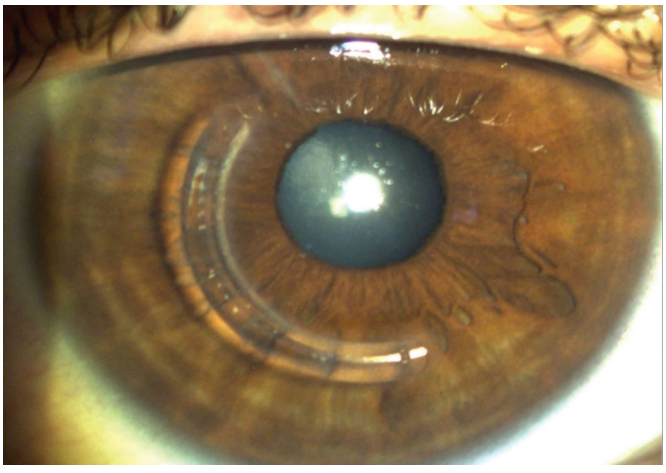

Fig. 7: Slit-lamp biomicroscopy of the right eye 6 weeks after femtosecond intracorneal ring segment

an extensive clinical examination was performed. The left eye remained stable with similar findings as reported in the first visit. The examination also included a scan using the Artemis very-high-frequency digital ultrasound scanner[40] (VHF-US; ArcScan Inc, Golden, CO, USA). Figures 9 and 10 present the VHF-US layered pachymetry data for the right and left eyes respectively.[40] In this analysis, epithelial, stromal, and total corneal thickness maps are presented along with the calculated standard deviation from normality of the epithelial and stromal thickness. In the right eye, a large arc can be seen temporally where the stromal thickness has increased due to the intracorneal ring segment. The distortion of the front surface of the stroma due to the ring is compensated for by epithelial remodeling with thinning to 44 µm directly over the ring and thickening to 99 µm adjacent to the ring.[41] In the left eye, the epithelial thickness profile appeared normal with slightly thinner epithelium superiorly as previously described for normal population.[42] The machine-based identification of keratoconus algorithm as described by Silverman et al[29] found the epithelial thickness for the left eye to be within the normal range. These data were in agreement with Pentacam HR, RTVue, and Placido-disk-based topography findings, which were found to be stable for the previous year. Orbscan (TECHNOLAS Perfect Vision; Munich, Germany) analysis was provided using the SCORE analyzer in the left eye (Fig. 11), with a score value of −0.5, which indicates negative for detecting ectasia.

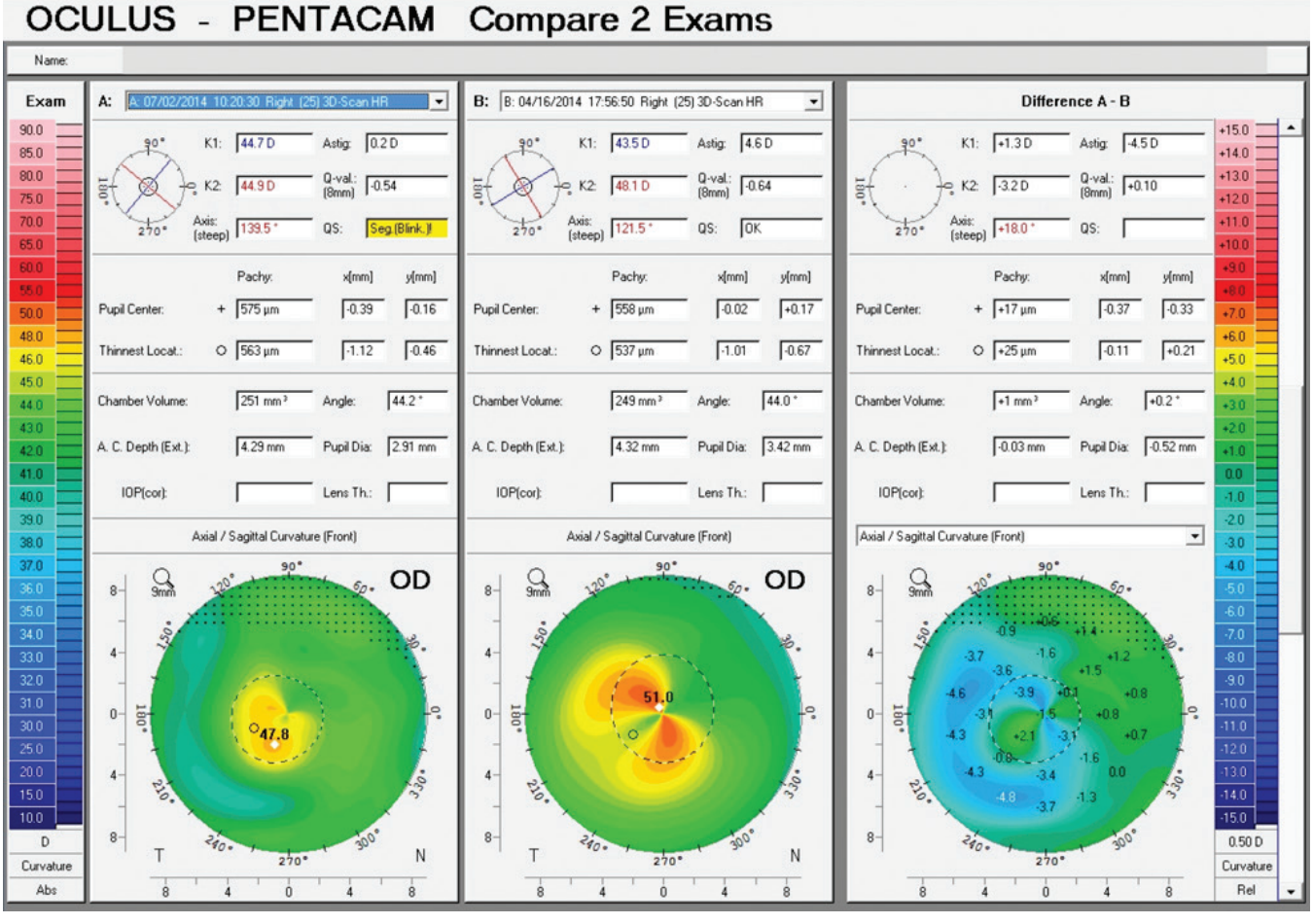

Fig. 8: Comparative corneal topography OD

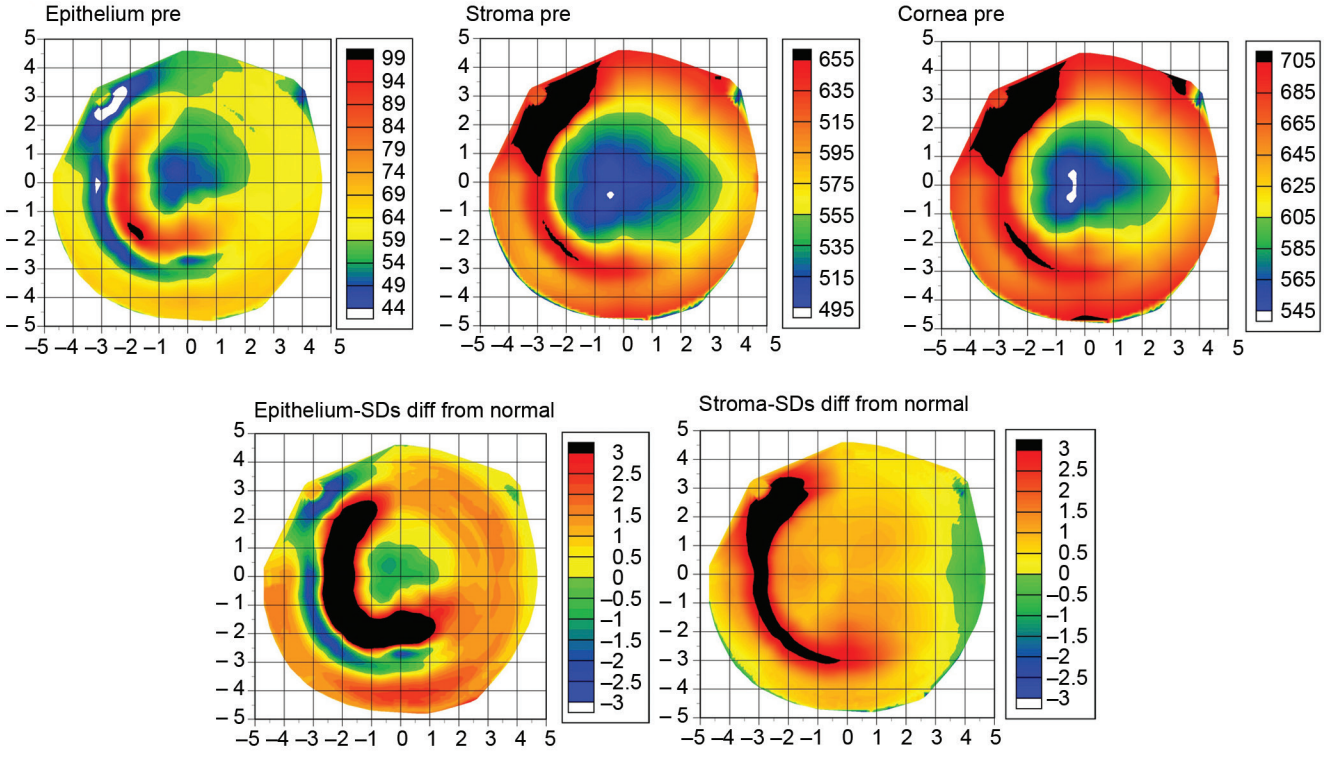

Fig. 9: Layered pachymetric mapping by very-high-frequency digital ultrasound from OD

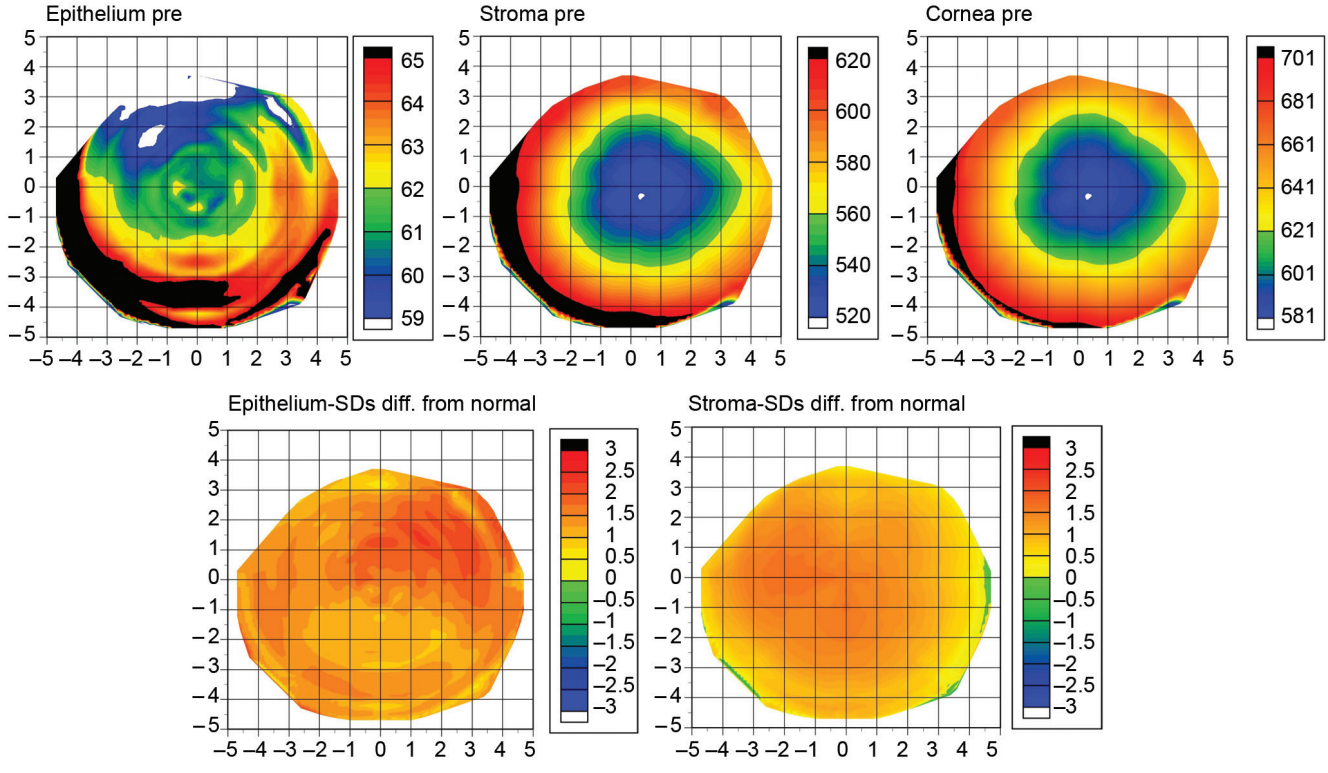

Fig. 10: Layered pachymetric mapping by very-high-frequency digital ultrasound from OS

Ocular biomechanical assessment was repeated with the ORA, finding CH and CRF of 10.3 and 10.2 mm Hg in the right eye and 12.2 and 12.0 mm Hg in the left eye. The ORA-KMI (keratoconus match index)[43] was 0.6 in the right eye and 0.69 in the left eye.

DISCUSSION

The diagnosis of very mild or subclinical ectatic corneal disease remains a relative challenge for corneal and refractive surgery specialists. In this context, the highly asymmetric cases present as a very interesting subgroup

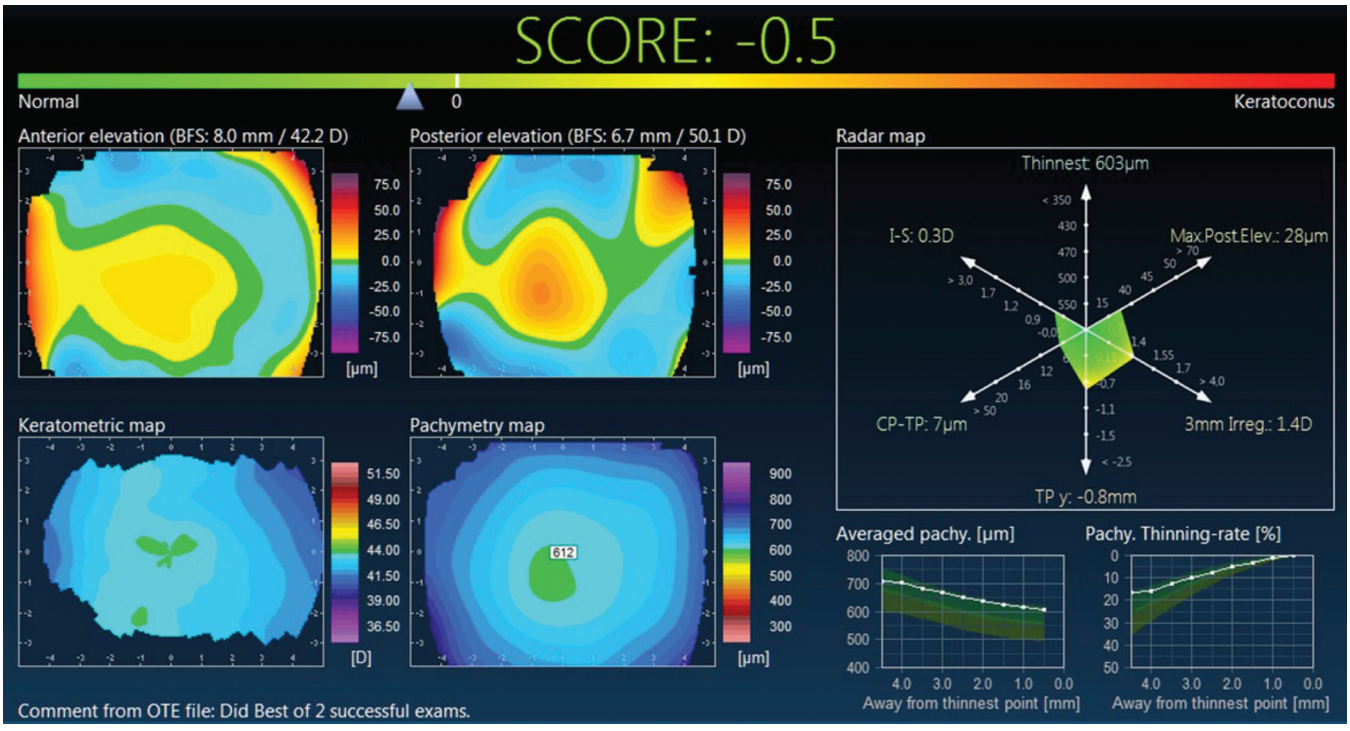

Fig. 11: SCORE analyzer from Orbscan

for diagnostic studies. However, while there was pan-American and global consensus that true unilateral keratoconus does not exist, there is also consensus that secondary (induced) ectasia, caused by a pure mechanical process, may occur unilaterally.[7,8] Thereby, some of the very asymmetric cases may actually have unilateral disease. This may raise a significant limitation for studies that involve very asymmetric ectasia cases for developing more advanced diagnostic methods for detecting mild ectatic disease before becoming apparent by front surface curvature changes.[21-26] However, the ideal study should consider longitudinal data, as previously done by Amsler in 1938.[10,44] In addition, the retrospective evaluation of cases that developed ectasia after refractive surgery should be deliberated, considering the preoperative corneal characteristics and the impact from the procedure, including having a residual stromal bed over 250 µm.[45] In fact, screening for ectasia risk prior to keratorefractive surgery aims to assess the amount of cornea susceptibility for biomechanical decompensation, not only detecting corneal ectatic diseases.[16]

This report illustrates and characterizes a unilateral corneal ectasia case. Advanced diagnostic methods, such as corneal tomography, have enabled the identification of subclinical ectatic diseases prior to loss of CDVA and other clinical signs that present late in the development of the disease.[46] Application of the most modern diagnostic techniques found no evidence for ectasia in the fellow left eye. While the limitations of subjective classification were highlighted in a previous study,[23] it is fundamental to go beyond front surface (topometric) evaluation for assessing ectasia risk or susceptibility. Corneal tomography refers to the three-dimensional reconstruction of corneal shape, characterizing front and back surface elevations, and corneal thickness distribution.[17] In this case, the left eye had rotating Scheimpflug[30,32] and slit-scanning[21] corneal tomography were unremarkably normal. In addition, epithelial thickness was within the normal range both by VHF-US and by spectral domain OCT,[42] Corvis ST deformation parameters were considered relatively normal, and biomechanical assessment from ORA was relatively normal and stable between examinations 1 year apart.[47] Clinical history provided fundamental information that the patient regularly rubbed his right eye, but did not rub his left eye. Therefore, the fact that the ectasia in the right eye could be explained by an external destabilizing environmental factor combined with the absence of any evidence for ectasia in the fellow eye indicates that the most likely diagnosis is secondary induced ectasia in the right eye (rather than asymmetric keratoconus with forme fruste disease), and that one would not expect the fellow eye to progress to ectasia without an equivalent external destabilizing event.

REFERENCES

1. Krachmer JH, Feder RS, Belin MW. Keratoconus and related noninflammatory corneal thinning disorders. Surv Ophthalmol 1984 Jan-Feb;28(4):293-322.
2. Rabinowitz YS. Keratoconus. Surv Ophthalmol 1998 Jan-Feb;42(4):297-319.

3. Holland DR, Maeda N, Hannush SB, Riveroll LH, Green MT, Klyce SD, Wilson SE. Unilateral keratoconus. Incidence and quantitative topographic analysis. Ophthalmology 1997 Sep;104(9):1409-1413.
4. Kennedy RH, Bourne WM, Dyer JA. A 48-year clinical and epidemiologic study of keratoconus. Am J Ophthalmol 1986 Mar 15;101(3):267-273.
5. Li X, Rabinowitz YS, Rasheed K, Yang H. Longitudinal study of the normal eyes in unilateral keratoconus patients. Ophthalmology 2004 Mar;111(3):440-446.
6. Rabinowitz YS, Nesburn AB, McDonnell PJ. Videokeratography of the fellow eye in unilateral keratoconus. Ophthalmology 1993 Feb;100(2):181-186.
7. Gomes JA, Tan D, Rapuano CJ, Belin MW, Ambrósio R Jr, Guell JL, Malecaze F, Nishida K, Sangwan VS. Group of Panelists for the Global Delphi Panel of Keratoconus and Ectatic Diseases. Global consensus on keratoconus and ectatic diseases. Cornea 2015 Apr;34(4):359-369.
8. Ambrósio R Jr, Belin MW, Perez VL, Abad JC, Gomes JAP. Definitions and concepts on keratoconus and ectatic corneal diseases: Panamerican Delphi Consensus – a pilot for the global consensus on ectasias. Int J Ker Ect Cor Dis 2014 Sep-Dec;3(3):99-106.
9. Klyce SD. Chasing the suspect: keratoconus. Br J Ophthalmol 2009 Jul;93(7):845-847.
10. Amsler M. [The "forme fruste" of keratoconus]. Wien Klin Wochenschr 1961 Dec 8;73:842-843.
11. Suzuki M, Amano S, Honda N, Usui T, Yamagami S, Oshika T. Longitudinal changes in corneal irregular astigmatism and visual acuity in eyes with keratoconus. Jpn J Ophthalmol 2007 Jul-Aug;51(4):265-269.
12. McGhee CN, Kim BZ, Wilson PJ. Contemporary treatment paradigms in keratoconus. Cornea 2015 Oct;34 (Suppl) 10: S16-S23.
13. Jafri B, Lichter H, Stulting RD. Asymmetric keratoconus attributed to eye rubbing. Cornea 2004 Aug;23(6):560-564.
14. Hawkes E, Nanavaty MA. Eye rubbing and keratoconus: a literature review. Int J Ker Ect Cor Dis 2014 Sep-Dec;3(3): 118-121.
15. Gordon-Shaag A, Millodot M, Shneor E, Liu Y. The genetic and environmental factors for keratoconus. Biomed Res Int 2015;2015:795738.
16. Ambrósio R Jr, Randleman JB. Screening for ectasia risk: what are we screening for and how should we screen for it? J Refract Surg 2013 Apr;29(4):230-232.
17. Ambrósio R Jr, Belin MW. Imaging of the cornea: topography vs tomography. J Refract Surg 2010 Nov;26(11):847-849.
18. Reinstein DZ, Gobbe M, Archer TJ, Silverman RH, Coleman DJ. Epithelial, stromal, and total corneal thickness in keratoconus: three-dimensional display with artemis very-high frequency digital ultrasound. J Refract Surg 2010 Apr;26(4): 259-271.
19. Reinstein DZ, Archer TJ, Gobbe M. Corneal epithelial thickness profile in the diagnosis of keratoconus. J Refract Surg 2009 Jul;25(7):604-610.
20. Li Y, Tan O, Brass R, Weiss JL, Huang D. Corneal epithelial thickness mapping by Fourier-domain optical coherence tomography in normal and keratoconic eyes. Ophthalmology 2012 Dec;119(12):2425-2433.
21. Saad A, Gatinel D. Topographic and tomographic properties of forme fruste keratoconus corneas. Invest Ophthalmol Vis Sci 2010 Nov;51(11):5546-5555.
22. Arbelaez MC, Versaci F, Vestri G, Barboni P, Savini G. Use of a support vector machine for keratoconus and subclinical keratoconus detection by topographic and tomographic data. Ophthalmology 2012 Nov;119(11):2231-2238.
23. Ramos IC, Correa R, Guerra FP, Trattler W, Belin MW, Klyce SD, Fontes BM, Schor P, Smolek MK, Dawson DG, et al. Variability of subjective classifications of corneal topography maps from LASIK candidates. J Refract Surg 2013 Nov;29(11):770-775.
24. Smadja D, Touboul D, Cohen A, Doveh E, Santhiago MR, Mello GR, Krueger RR, Colin J. Detection of subclinical keratoconus using an automated decision tree classification. Am J Ophthalmol 2013 Aug;156(2):237-246.e1.
25. Fontes BM, Ambrósio R Jr, Salomao M, Velarde GC, Nose W. Biomechanical and tomographic analysis of unilateral keratoconus. J Refract Surg 2010 Sep;26(9):677-681.
26. Steinberg J, Katz T, Lucke K, Frings A, Druchkiv V, Linke SJ. Screening for keratoconus with new dynamic biomechanical *in vivo* scheimpflug analyses. Cornea 2015 Nov;34(11):1404-1412.
27. Reinstein DZ, Archer TJ, Urs R, Gobbe M, RoyChoudhury A, Silverman RH. Detection of keratoconus in clinically and algorithmically topographically normal fellow eyes using epithelial thickness analysis. J Refract Surg 2015 Nov;31(11):736-744.
28. Li Y, Meisler DM, Tang M, Lu AT, Thakrar V, Reiser BJ, Huang D. Keratoconus diagnosis with optical coherence tomography pachymetry mapping. Ophthalmology 2008 Dec;115(12): 2159-2166.
29. Silverman RH, Urs R, Roychoudhury A, Archer TJ, Gobbe M, Reinstein DZ. Epithelial remodeling as basis for machine-based identification of keratoconus. Invest Ophthalmol Vis Sci 2014 Mar13;55(3):1580-1587.
30. Ambrósio R Jr, Valbon BF, Faria-Correia F, Ramos I, Luz A. Scheimpflug imaging for laser refractive surgery. Curr Opin Ophthalmol 2013 Jul;24(4):310-320.
31. Chan C, Ang M, Saad A, Chua D, Mejia M, Lim L, Gatinel D. Validation of an objective scoring system for forme fruste keratoconus detection and post-LASIK ectasia risk assessment in asian eyes. Cornea 2015 Sep;34(9):996-1004.
32. Correia FF, Ramos IC, Lopes B, Salomão MQ, Luz A, Correa RO, Belin MW, Ambrósio R Jr. Topometric and tomographic indices for the diagnosis of keratoconus. Int J Kerat Ect Cor Dis 2012 May-Aug;1(2):92-99.
33. Salomao MQ, Guerra FP, Ramos IC, Jordao LF, Canedo ALC, Valbon BF, Luz A, Correa R, Lopes B, Ambrósio R Jr. Accuracy of topometric indices for distinguishing between keratoconic and normal corneas. Int J Kerat Ect Cor Dis 2013 Sep-Dec;2(3):108-112.
34. Belin MW, Ducan J, Ambrósio R Jr, Gomes JAP. A new tomographic method of staging/classifying keratoconus: the ABCD grading system. Int J Kerat Ect Cor Dis 2015 Sep-Dec;4(3):55-63.
35. Ambrósio R Jr, Alonso RS, Luz A, Coca Velarde LG. Corneal-thickness spatial profile and corneal-volume distribution: tomographic indices to detect keratoconus. J Cataract Refract Surg 2006 Nov;32(11):1851-1859.
36. Ambrósio R Jr, Caiado AL, Guerra FP, Louzada R, Roy AS, Luz A, Dupps WJ, Belin MW. Novel pachymetric parameters based on corneal tomography for diagnosing keratoconus. J Refract Surg 2011 Oct;27(10):753-758.
37. Luce DA. Determining *in vivo* biomechanical properties of the cornea with an ocular response analyzer. J Cataract Refract Surg 2005 Jan;31(1):156-162.

38. Ambrósio R Jr, Ramos I, Luz A, Faria FC, Steinmueller A, Krug M, Belin MW, Roberts CJ. Dynamic ultra high speed Scheimpflug imaging for assessing corneal biomechanical properties. Rev Bras Oftalmol 2013 Mar/Apr;72(2):99-102.
39. Kerautret J, Colin J, Touboul D, Roberts C. Biomechanical characteristics of the ectatic cornea. J Cataract Refract Surg 2008 Mar;34(3):510-513.
40. Reinstein DZ, Silverman RH, Raevsky T, Simoni GJ, Lloyd HO, Najafi DJ, Rondeau MJ, Coleman DJ. Arc-scanning very high-frequency digital ultrasound for 3D pachymetric mapping of the corneal epithelium and stroma in laser in situ keratomileusis. J Refract Surg 2000 Jul-Aug;16(4):414-430.
41. Reinstein DZ, Srivannaboon S, Holland SP. Epithelial and stromal changes induced by intacs examined by three-dimensional very high-frequency digital ultrasound. J Refract Surg 2001 May-Jun;17(3):310-318.
42. Reinstein DZ, Archer TJ, Gobbe M, Silverman RH, Coleman DJ. Epithelial thickness in the normal cornea: three-dimensional display with Artemis very high-frequency digital ultrasound. J Refract Surg 2008 Jun;24(6):571-581.
43. Labiris G, Giarmoukakis A, Gatzioufas Z, Sideroudi H, Kozobolis V, Seitz B. Diagnostic capacity of the keratoconus match index and keratoconus match probability in subclinical keratoconus. J Cataract Refract Surg 2014 Jun;40(6):999-1005.
44. Amsler M. Le keratocone fruste au javal. Ophthalmologica. J Int D'ophtalmol Int J Ophthalmol. Zeitschrift fur Augenheilkunde 1938/1939;96:77-83.
45. Ambrósio R Jr, Ramos I, Lopes B, Canedo ALC, Correa R, Guerra F, Luz A, Price FW Jr, Price MO, Schallhor S, et al. Assessing ectasia susceptibility prior to LASIK: the role of age and residual stromal bed (RSB) in conjunction to Belin-Ambrósio deviation index (BAD-D). Rev Bras Oftalmol 2014 Mar/Apr;73(2):75-80.
46. Maeda N, Klyce SD, Tano Y. Detection and classification of mild irregular astigmatism in patients with good visual acuity. Surv Ophthalmol 1998 Jul-Aug;43(1):53-58.
47. Fontes BM, Ambrósio R Jr, Jardim D, Velarde GC, Nose W. Corneal biomechanical metrics and anterior segment parameters in mild keratoconus. Ophthalmology 2010 Apr;117(4):673-679.